Inorg. Chem. **2006**, *45*, 1972–1977

A New Type of Hybrid Magnetic Semiconductor Based upon Polymeric Iodoplumbate and Metal–Organic Complexes as Templates

Zhang-Jing Zhang,[†,‡] Sheng-Chang Xiang,[†] Yong-Fan Zhang,[§] A-Qing Wu,[†] Li-Zhen Cai,[†] Guo-Cong Guo,*[,†] and Jin-Shun Huang[†]

State Key Laboratory of Structural Chemistry, Fujian Institute of Research on the Structure of Matter, Chinese Academy of Sciences, Fuzhou, Fujian 350002, People's Republic of China, Graduate School of Chinese Academy of Sciences, Beijing 100039, People's Republic of China, and Department of Chemistry, Fuzhou University, Fuzhou, Fujian 350002, People's Republic of China

Received August 7, 2005

A new type of one-dimensional organic–inorganic hybrid $[M(en)_3]Pb_2I_6$ [M = Mn (**1**), Fe (**2**), Zn (**3**), Ni (**4**); en = ethylenediamine] has been obtained and structurally characterized by X-ray crystallography, which opens a new approach to construct hybrid magnetic semiconductors. The results of optical absorption spectra and theoretical calculations for compounds **1**–**3** reveal a quantum confinement effect, and the variable-temperature magnetic susceptibility measurements for **1**, **2**, and **4** indicate ferromagnetic, antiferromagnetic, and paramagnetic behavior, respectively.

Introduction

Organic−inorganic hybrids are likely to exhibit diverse structures, improved properties, and functions unobserved in purely inorganic or organic phases, such as novel magnetic,[1] electrical,[2] and optical properties,[3] which provide great possibilities to construct attractive multifunctionality in one material. Among the numerous hybrid materials, the magnetic molecular conductors mixing magnetism with conductivity have attracted great attention and are expected to provide new ingredients in electronic molecular devices.[4] Coronado and Day have pointed out that the combination of magnetic moments with conduction electrons in one hybrid may give rise to a simple superposition of magnetic and conducting properties if the two compositions are electronically independent or to a mutual influence between these properties if they interact.[4c] Past studies in this field are concentrated on the hybrids based on organic conductors, for example, tetrathiafulvalene (TTF) and its derivatives, in which the counterions employ the magnetic transition-metal complexes including metal halides $[MX_4]^{2-}$ (X = halide),[5] pseudohalides $[M(CN)_6]^{3-}$,[6] MPS_3,[4d,7] trioxalato transition-metal complexes $[M(C_2O_4)_3]^{3-}$ and $[M^{II}M^{III}(C_2O_4)_3]^-$,[8] and poly(oxometalate) clusters.[9] Our interest is to design and construct novel magnetic semiconductors by the hybrids of inorganic semiconductors instead of organic conductors and magnetic metal−organic complexes as shown in Figure 1b.

It is well-known that metal halides such as PbX_2 and SnX_2 (X = Cl, Br, and I) have been widely studied as semicon-

* To whom correspondence should be addressed. E-mail: gcguo@ms.fjirsm.ac.cn.

† Fujian Institute of Research on the Structure of Matter, Chinese Academy of Sciences.

‡ Graduate School of Chinese Academy of Sciences.

§ Fuzhou University.

(1) (a) Day, P. *Trans. R. Soc. London, Ser. A* **1985**, *314*, 145. (b) Mitzi, D. B.; Field, C. A.; Schlesinger, Z.; Laibowitz, R. B. *J. Solid State Chem.* **1995**, *114*, 159. (c) Kurmoo, M. *J. Mater. Chem.* **1999**, *9*, 2595.

(2) (a) Papavassiliou, G. C.; Koutelas, I. B.; Terzis, A.; Whangbo, M. H. *Solid State Commun.* **1994**, *91*, 695. (b) Mitzi, D. B.; Wang, S.; Field, C. A.; Chess, C. A.; Guloy, A. M. *Science* **1995**, *267*, 473. (c) Gomez-Romero, P.; Chojak, M.; Cuentas-Gallegos, K.; Asensio, J. A.; Kulesza, P. J.; Casan-Pastor, N.; Lira-Cantu, M. *Electrochem. Commun.* **2003**, *5*, 149.

(3) (a) Ishihara, T.; Goto, T. In *Nonlinear Optics of Organics and Semiconductors*; Kobayashi, T., Ed.; Springer-Verlag: Berlin, 1989; Vol. 36, p 72. (b) Ishihara, T.; Takahashi, J.; Goto, T. *Phys. Rev. B* **1990**, *42*, 11099. (c) Calabrese, J.; Jones, N. L.; Harlow, R. L.; Thorn, D.; Wang, Y. *J. Am. Chem. Soc.* **1991**, *113*, 2328.

(4) (a) Day, P.; Kurmoo, M.; Mallah, T.; Marsden, I. R.; Friend, R. H.; Pratt, F. L.; Hayes, W.; Chasseau, D.; Gaultier, J.; Bravic, G.; Ducasse, L. *J. Am. Chem. Soc.* **1992**, *114*, 10722. (b) Gomez-Garcia, C. J.; Ouahab, L.; Gimenez, C.; Triki, S.; Coronado, E.; Delhaes, P. *Angew. Chem., Int. Ed. Engl.* **1994**, *33*, 223. (c) Coronado, E.; Day, P. *Chem. Rev.* **2004**, *104*, 5419 and references cited therein. (d) Rabu, P.; Drillon, M. *Adv. Eng. Mater.* **2003**, *5*, 189. (e) Ouahab, L. *Chem. Mater.* **1997**, *9*, 1909.

(5) (a) Ojima, E.; Fujiwara, H.; Kato, K.; Kobayashi, H. *J. Am. Chem. Soc.* **1999**, *121*, 5581. (b) Fujiwara, H.; Kobayashi, H.; Fujiwara, E.; Kobayashi, A. *J. Am. Chem. Soc.* **2002**, *124*, 6816. (c) Kobayashi, H.; Tomita, H.; Naito, T.; Kobayashi, A.; Sakai, F.; Watanabe, T.; Cassoux, P. *J. Am. Chem. Soc.* **1996**, *118*, 368.

10.1021/ic051350v CCC: $33.50
Published on Web 02/01/2006

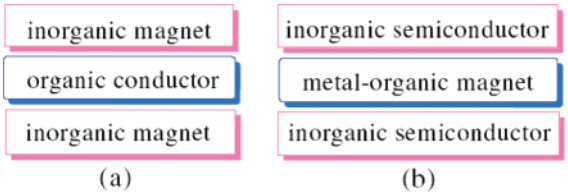

Figure 1. Schematic arrangements of an organic−inorganic magnetic conductor (a) and an organic−inorganic magnetic semiconductor (b).

ducting components in the field of organic−inorganic hybrid semiconductors,[10] which have demonstrated potential applications in display and storage technologies because of their stable exciton, excellent film processability, and superior carrier mobility.[11] Recently, Batail and co-workers have obtained PbI_2-based hybrid conductors through the insertion of conducting β-(EDT−TTF−I_2), where EDT = ethylenediaminetetraacetic acid.[12] Most works are focused on the introduction of protonated organic amine into the metal halides,[13] and only two structures of two-dimensional (2-D) metal−organic complex templated hybrids based on $PbCl_2$ or $PbBr_2$ have been reported before.[14] However, the stems on coinstantaneous magnetic and semiconducting properties existing in such hybrids have not been investigated. It is desirable to coassemble the inorganic semiconductor iodoplumbate with a magnetic metal complex to form a new type of magnetic semiconductor. Herein, we report a new series of hybrid magnetic semiconductors $[M(en)_3]Pb_2I_6$ [M = Mn (**1**), Fe (**2**), Zn (**3**), Ni (**4**)] containing iodoplumbate chains and $M(en)_3^{2+}$ ions, in which the study of coexisting magnetic and semiconducting properties in one compound among an iodoplumbate and iodostannate system has been demonstrated for the first time.

Experimental Section

Materials and Methods. All chemicals were used as purchased without further purification. Four title compounds were prepared under solvothermal conditions in a 25-mL Teflon-lined steel autoclave under autogenous pressure. Thermogravimetric analysis (TGA) and differential scanning calorimetry were performed on a Netzsch Sta449C thermoanalyzer under a N_2 atmosphere in the range of 40−750 °C at a heating rate of 15 °C/min. Optical diffuse-reflectance spectra were measured on a PE Lambda 35 UV−vis spectrophotometer equipped with an integrating sphere at 293 K, and the $BaSO_4$ plate was used as the reference. The values of E_g were obtained with the use of a straightforward extrapolation method.[15] Magnetic studies were performed with a PPMS-9T magnetometer. A diamagnetic correction was estimated from Pascal's constants.[16] The temperature dependence of the magnetic susceptibilities for **1**, **2**, and **4** was investigated over the temperature range of 2−300 K under a magnetic field of 5000 G.

Computational Descriptions. The crystallographic data of **1**−**3** determined by the X-ray and edge-sharing octahedral structure of bulk PbI_2[17] were used to calculate electronic band structures of the solid compounds. The ab initio calculations of the band structures were performed by the computer code *CASTEP*.[18] This code employs density functional theory using a plane-wave basis set with Vanderbilt ultrasoft pseudopotentials[19] to approximate the interactions between core and valence electrons. The exchange-correlation energy was calculated using the Perdew−Burke−Ernzerhof modification to the generalized gradient approximation.[20] A kinetic-energy cutoff of 280 eV was used throughout our work. Pseudo

(6) (a) Clemente-Leon, M.; Coronado, E.; Galan-Mascaros, J. R.; Gimenez-Saiz, C.; Gomez-Garcia, C. J.; Fabre, J. M. *Synth. Met*. **1999**, *103*, 2279. (b) Clemente-Leon, M.; Coronado, E.; Galan-Mascaros, J. R.; Gimenez-Saiz, C.; Gomez-Garcia, C. J.; Ribera, E.; Vidal-Gancedo, J.; Rovira, C.; Canadell, E.; Lauhkin, V. *Inorg. Chem.* **2001**, *40*, 3526. (c) Shibaeva, R. P.; Yagubskii, E. B.; Canadell, E.; Khasanov, S. S.; Zorina, L. V.; Kushch, L. A.; Prokhorova, T. G.; Shevyakova, I. Yu., Buravov, L. I.; Tkacheva, V. A.; Gener, M. *Synth. Met.* **2003**, *133*, 373. (d) Zorina, L. V.; Khasanov, S. S.; Shibaeva, R. P.; Gener, M.; Rousseau, R.; Canadell, E.; Kushch, L. A.; Yagubskii, E. B.; Drozdova, O. O.; Yakushi, K. *J. Mater. Chem*. **2000**, *10*, 2017.

(7) (a) Lacroix, P.; Audiere, J. P.; Clement, R. *Chem. Commun.* **1989**, 536. (b) Floquet, S.; Salunke, S.; Boillot, M.; Clement, R.; Varret, F.; Boukheddaden, K.; Riviere, E. *Chem. Mater*. **2002**, *14*, 4164. (c) Leaustic, A.; Riviere, E.; Clement, R. *Chem. Mater*. **2003**, *15*, 4784. (d) Lomas, L.; Lacroix, P.; Audiere, J. P.; Clement, R. *J. Mater. Chem.* **1991**, *1*, 475. (e) Koseoglu, Y.; Yildiz, F.; Yakhmi, J. V.; Qin, J.; Chen, X.; Aktas, B. *J. Magn. Magn. Mater.* **2003**, *258*−*259*, 416. (f) Clement, R.; Leaustic, A. In *Magnetism: Molecules to Materials II*; Wiley-VCH: Weinheim, Germany, 2001; p 397 and references cited therein.

(8) (a) Kurmoo, M.; Graham, A. W.; Day, P.; Coles, S. J.; Hurtshouse, M. B.; Caulfield, J. L.; Singleton, J.; Pratt, F. L.; Hayes, W.; Ducasse, L.; Guionneau, P. *J. Am. Chem. Soc*. **1995**, *117*, 12209. (b) Coronado, E.; Galan-Mascaros, J. R.; Gomez Garcia, C. J. *J. Chem. Soc., Dalton Trans*. **2000**, 205. (c) Prokhorova, T. G.; Khasanov, S. S.; Zorina, L. V.; Buravov, L. I.; Tkacheva, V. A.; Baskakov, A. A.; Morgunov, R. B.; Gener, M.; Canadell, E.; Shibaeva, R. P.; Yagubskii, E. B. *Adv. Funct. Mater*. **2003**, *13*, 403. (d) Audouard, A.; Laukhin, V. N.; Brossard, L.; Prokhorova, T. G.; Yaguhskii, E. B. *Phys. Rev B* **2004**, *69*, 144523. (e) Coronado, E.; Galan-Mascaros, J. R.; Gomez-Garcia, C. J.; Laukhin, V. *Nature* **2000**, *408*, 447.

(9) (a) Llusar, R.; Uriel, S.; Vicent, C.; Clemente-Juan, J. M.; Coronado, E.; Gomez-Garcia, C. J.; Braida, B.; Canadell, E. *J. Am. Chem. Soc.* **2004**, *126*, 12076. (b) Coronado, E.; Galan-Mascaros, J. R.; Gimenez-Saiz, C.; Gomez-Garcia, C. J.; Triki, S. *J. Am. Chem. Soc*. **1998**, *120*, 4671. (c) Galan-Mascaros, J. R.; Gimenez-Saiz, C.; Triki, S.; Gomez-Garcia, C. J.; Coronado, E.; Ouahab, L. *Angew. Chem., Int. Ed. Engl*. **1995**, *34*, 1460. (d) Ouahab, L.; Bencharif, M.; Mhanni, A.; Pelloquin, D.; Halet, J.-F.; Pena, O.; Padiou, J.; Grandjean, D. *Chem. Mater*. **1992**, *4*, 666.

(10) (a) Xu, Z. T.; Mitzi, D. B. *Inorg. Chem*. **2003**, *42*, 6589. (b) Kuntson, J. L.; Martin, J. D.; Mitzi, D. B. *Inorg. Chem*. **2005**, *44*, 4699. (c) Mitzi, D. B. *IBM J. Res. Dev.* **2001**, *45*, 1. (d) Mitzi, D. B. *Prog. Inorg. Chem*. **1999**, *48*, 1.

(11) Kagan, C. R.; Mitzi, D. B.; Dimitrakopoulos, C. D. *Science* **1999**, *286*, 945.

(12) (a) Devic, T.; Evain, M.; Moelo, Y.; Canadell, E.; Auban-Senzier, P.; Fourmingue, M.; Batail, P. *J. Am. Chem. Soc*. **2003**, *125*, 3295. (b) Devic, T.; Canadell, E.; Auban-Senzier, A.; Batail, P. *J. Mater. Chem*. **2004**, *14*, 135. (c) Olejniczak, I.; Gromadzinski, B.; Graja, A.; Devic, T.; Batail, P. *Mater. Soc*. **2004**, *22*, 347.

(13) (a) Tang, Z. J.; Guloy, A. M. *J. Am. Chem. Soc.* **1999**, *121*, 452. (b) Corradi, A. B.; Ferrari, A. M.; Pellacani, G. C.; Saccani, A.; Sandrolini, F.; Sgarabotto, P. *Inorg. Chem*. **1999**, *38*, 716. (c) Mousdis, G. A.; Gionis, V.; Papavassiliou, G. C.; Raptopoulou, C. P.; Terzis, A. *J. Mater. Chem*. **1998**, *8*, 2259. (d) Krautscheid, H.; Lode, C.; Vielsack, F.; Vollmer, H. *J. Chem. Soc., Dalton Trans.* **2001**, 1099. (e) Mercier, N.; Poiroux, S.; Riou, A.; Batail, P. *Inorg. Chem*. **2004**, *43*, 8361.

(14) (a) Mercier, N.; Riou, A. *Chem. Commun*. ***2004***, 844. (b) Aquilino, A.; Cannas, M.; Christini, A.; Marongiu, G. *Chem. Commun.* **1978**, 347.

(15) (a) Wendlandt, W. W.; Hecht, H. G. *Reflectance Spectroscopy*; Interscience Publishers: New York, 1966. (b) Kotiim, G. *Reflectance Spectroscopy*; Springer-Verlag: New York, 1969. (c) Schevciw, O.; White, W. B. *Mater. Res. Bull*. **1983**, *18*, 1059.

(16) Kahn, O. *Molecular Magnetism*; VCH: Weinheim, Germany, 1993.

(17) The structure of PbI_2 is adopted from: Agrawal, V. K.; Chadha, G. K.; Trigunayat, G. C. *Acta Crystallogr., Sect. A* **1970**, *26*, 140.

(18) (a) Segall, M. D.; Lindan, P. L. D.; Probert, M. J.; Pickard, C. J.; Hasnip, P. J.; Clark, S. J.; Payne, M. C. *J. Phys.: Condens. Matter* **2002**, *14*, 2717. (b) Segall, M.; Lindan, P.; Probert, M.; Pickard, C.; Hasnip, P.; Clark, S.; Payne, M. *Materials Studio CASTEP*, version 2.2, 2002.

(19) Vanderbilt, D. *Phys. Rev. B* **1990**, *41*, 7892.

(20) Perdew, J. P.; Burke, K.; Ernzerhof, M. *Phys. Rev. Lett.* **1996**, *77*, 3865.

Table 1. Crystal and Structure Refinement Data for **1**−**4**

	1	**2**	**3**	**4**
formula	$C_6H_{24}I_6MnN_6Pb_2$	$C_6H_{24}FeI_6N_6Pb_2$	$C_6H_{24}I_6N_6Pb_2Zn$	$C_6H_{24}I_6N_6NiPb_2$
M_r	1411.03	1411.94	1421.46	1414.80
cryst size (mm^3)	0.50 × 0.50 × 0.48	0.40 × 0.30 × 0.20	0.18 × 0.18 × 0.10	0.10 × 0.10 × 0.10
cryst syst	monoclinic	monoclinic	monoclinic	monoclinic
space group	*C*2/*c*	*C*2/*c*	*C*2/*c*	*C*2/*c*
a (Å)	12.887(9)	12.867(3)	12.920(2)	12.9194(19)
b (Å)	24.800(9)	24.472(6)	24.474(5)	24.305(3)
c (Å)	8.865(7)	8.8642(13)	8.9493(15)	8.9589(13)
β (deg)	144.10(9)	114.101(1)	114.271(13)	114.595(2)
V ($Å^3$)	2586(3)	2545.6(9)	2579.6(8)	2557.9(6)
D_{calcd} (Mg/m^3)	3.624	3.684	3.660	3.674
Z	4	4	4	4
F(000)	2436	2440	2456	2448
abs coeff (mm^{-1})	20.633	21.036	21.126	21.103
reflns collcd/unique (R_{int})	8088/2278 (0.0868)	9239/2237 (0.0687)	2422/2276 (0.0302)	8396/2267 (0.0419)
data/params/restraints	1952/102/0	2023/106/0	1749/101/1	1999/100/0
R1	0.0461	0.0272	0.0393	0.0383
wR2	0.1010	0.0621	0.0804	0.1050
GOF on F^2	1.045	1.050	1.011	1.008
$\Delta\rho_{max}$ and $\Delta\rho_{min}$ ($e/Å^3$)	2.063 and −2.078	1.072 and −1.319	0.932 and −1.615	2.608 and −1.050

atomic calculations were performed for H $1s^1$, C $2s^22p^2$, N $2s^22p^3$, I $5s^25p^5$, Pb $5d^{10}6s^26p^2$, Fe $3d^64s^2$, Mn $3d^54s^2$, and Zn $3d^{10}4s^2$. The smearing width for the density of states (DOS) is 0.05 eV. The other calculating parameters and convergent criteria were set by the default values of the *CASTEP* code. The calculations of the linear optical properties described in terms of the complex dielectric function $\epsilon = \epsilon_1 + \epsilon_2$ were also made in this work. The imaginary part of the dielectric function $\epsilon_2(\omega)$ was given in the following equation:[21]

$$\epsilon_2(\omega) = 4(\pi e/m\omega)^2 \sum_{V,C} \int_{BZ} 2d\mathbf{k}/(2\pi)^3 |\mathbf{e}\cdot\mathbf{M}_{CV}(\mathbf{k})|^2 \delta(E_C(\mathbf{k}) - E_V(\mathbf{k}) - \hbar\omega)$$

The symbol $\sum$ is the summation over the valence (V) and conduction (C) bands, and the symbol $\int$ is integration over **k** vectors in the Brillouin zone (BZ). $\mathbf{e}\cdot\mathbf{M}_{CV}(\mathbf{k})$ is an electron transition moment between the conduction and valence bands at the **k** point, and the argument of the δ function is the energy difference between the conduction and valence bands at the **k** point with absorption of a quantum $\hbar\omega$ $[E_C(\mathbf{k}) - E_V(\mathbf{k}) - \hbar\omega]$.

Crystal Structure Analyses. The intensity data sets of **1**, **2**, and **4** were collected on a Rigaku Mercury CCD diffractometer equipped with graphite-monochromated Mo Kα radiation (λ = 0.710 73 Å) using an ω-scan technique at 293 K, and the intensity data set of **3** was collected on a Rigaku AFC7R diffractometer equipped with graphite-monochromated Mo Kα radiation (λ = 0.710 73 Å) using $\omega-2\theta$-scan technique at 293 K. The data sets were reduced by *CrystalClear* and *CrystalStructure* programs.[22] The structures were solved by direct methods using the Siemens *SHELXTL*, version 5, package of crystallographic software.[23] The difference Fourier maps based on these atomic positions yield the other non-H atoms. The structures were refined using full-matrix least-squares refinement on F^2. The H atoms were allowed to ride on their respective parent atoms and included in the structure factor calculations with assigned isotropic thermal parameters, except for the H atoms of the disordered C atoms and the C and N atoms connected with the disordered C atoms. Crystallographic data and structural refinements for **1**−**4** are summarized in Table 1.

Synthesis of $[Mn(en)_3]Pb_2I_6$ (1). A mixture of PbI_2 (0.5 mmol, 231 mg) and $MnCl_2\cdot4H_2O$ (0.5 mmol, 99 mg) was heated with en (15 mmol, 1 mL), HI acid (≥45%, 3 mL), and ethanol (2 mL) at 180 °C for 2 days. Upon cooling at 3 °C/h to room temperature, yellow prismatic crystals of **1** were obtained in 80% yield (based on PbI_2). The crystals were collected by filtration and washed with ethanol. Elem anal. Calcd for $C_6H_{24}I_6MnN_6Pb_2$: H, 1.71; C, 5.11; N, 5.96. Found: H, 1.75; C, 5.15; N, 5.91.

Synthesis of $[Fe(en)_3]Pb_2I_6$ (2). Compound **2** was prepared under conditions similar to those of **1** with $FeCl_2$ (0.5 mmol, 64 mg) instead of $MnCl_2\cdot4H_2O$ in **1**. Yield: 50% (based on PbI_2). Elem anal. Calcd for $C_6H_{24}FeI_6N_6Pb_2$: H, 1.71; C, 5.10; N, 5.95. Found: H, 1.70; C, 5.18; N, 5.90.

Synthesis of $[Zn(en)_3]Pb_2I_6$ (3). Compound **3** was prepared under conditions similar to those of **1** with $ZnCl_2$ (0.5 mmol, 68 mg) instead of $MnCl_2\cdot4H_2O$ in **1**. Yield: 83% (based on PbI_2). Elem anal. Calcd for $C_6H_{24}I_6N_6Pb_2Zn$: H, 1.70; C, 5.07; N, 5.91. Found: H, 1.65; C, 5.12; N, 5.89.

Synthesis of $[Ni(en)_3]Pb_2I_6$ (4). Compound **4** was prepared under conditions similar to those of **1** with $NiCl_2\cdot6H_2O$ (0.5 mmol, 119 mg) instead of $MnCl_2\cdot4H_2O$ in **1**. Yield: 70% (based on PbI_2). Elem anal. Calcd for $C_6H_{24}I_6N_6NiPb_2$: H, 1.71; C, 5.09; N, 5.94. Found: H, 1.70; C, 5.08; N, 5.95.

Results and Discussion

Synthetic Considerations. Four isomorphous compounds were obtained by similar reaction procedures except using different transition-metal halides. Although the solvothermal method has been widely used in the syntheses of organic−inorganic hybrids to obtain new compounds with novel structures and properties, it has scarcely been used in the haloplumbate-based hybrid system. The solvothermal condition is indispensable for the syntheses of the title compounds, while the crystals of four compounds cannot be obtained under the condition of refluxing mixtures. In the processes of these reactions, the reaction temperature plays an important role. The crystals of the title compounds cannot be obtained if the reaction temperature decreases to 120 °C. At the same

(21) Bassani, F.; Parravicini, G. P. *Electronic States and Optical Transitions in Solids*; Pergamon Press Ltd.: Oxford, U.K., 1975; pp 149−154.
(22) (a) Rigaku mercury CCD diffractometer: Rigaku. *CrystalClear*, version 1.35; Rigaku Corp.: Tokyo, Japan, 2001. (b) Rigaku AFC7R diffractometer: Rigaku. *CrystalStructure*, version 3.10; Rigaku Corp. and Rigaku/MSC: Tokyo, Japan, 2002.
(23) *SHELXTL Reference Manual*, version 5; Siemens Energy & Automation: Madison, WI, 1994.

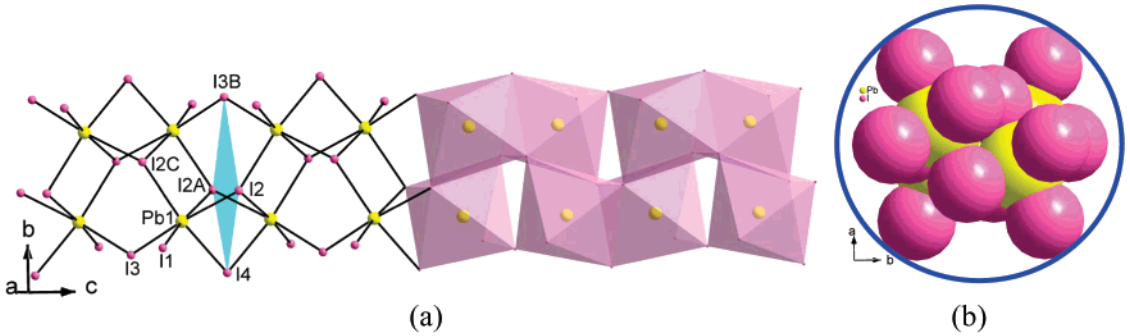

Figure 2. (a) Fragment of the $(Pb_2I_6)_n^{2n-}$ anion in **1** extending along the *c* axis. (b) Space-filling mode of the $(Pb_2I_6)_n^{2n-}$ chain in **1** viewed down the *c* axis. Symmetry codes: A = $-x$, $1-y$, $^1/_2-z$; B = $-x$, $1-y$, $-z$; C = x, $1-y$, $^1/_2+z$.

time, it is important to keep a large excess of en in the reactive system, with the pH value being about 8.0. When the molar ratio of MCl_2 and en decreases to 1:15 or lower, no desirable crystals were obtained.

Crystal Structures. The present compounds are isomorphous, and the structure of **1** is discussed in detail. Compound **1** is composed of $Mn(en)_3^{2+}$ complexes and infinite $(Pb_2I_6)_n^{2n-}$ double chains with face-sharing bi-octahedra Pb_2I_9 as the building unit. The bi-octahedra corner-share with each other through I3 atoms to form a single octahedral chain, which further connects with its symmetry-related chain through edge sharing of their octahedra to form a double chain extending along the *c* axis, as shown in Figure 2a. Unlike the double chain in the title compounds, the connection among the octahedra of the double chain in $(C_6H_{10}N_2)Pb_2I_6$ is edge-sharing.[24] It is noteworthy that the diameters of the section of double chain in **1**−**4** are about 1.41 nm, representing a nanowire as shown in Figure 2b. There is a noncrystallographic mirror plane defined by the I2, I2A, I3B, and I4 atoms, indicating that the molecular structure of **1** has a higher symmetry than the analogue of $[C_3H_7N(C_2H_4)NC_3H_7](Pb_2I_6)$,[13d] in which no symmetry operation transforms two PbI_6 into each other because of space group differences dictated by the organic captions. The Pb atom is in a slightly distorted octahedral coordination environment, with the Pb−I bond lengths varying from 3.006(3) to 3.452(4) Å and an axial I2C−Pb−I4 bond angle of 172.197(19)°. The $(Pb_2I_6)_n^{2n-}$ chains are surrounded by six columns of $[Mn(en)_3]^{2+}$ ions to form a crystal structure (Figure S2 in the Supporting Information). The configuration of discrete $[M(en)_3]^{2+}$ cations in the present compounds is $\Lambda(\lambda\lambda\lambda)$ or $\Delta(\delta\delta\delta)$ according to Saito's description.[25] The Mn···Mn, Fe···Fe, Zn···Zn, and Ni···Ni distances are 8.87, 8.86, 8.95, and 8.96 Å, respectively.

Thermal Properties. TGA (Figure S1 of the Supporting Information) of **1**−**3** revealed that they all started to decompose at a temperature of about 270 °C and in one distinct step with weight changes of about 12.8% before about 480 °C, which correspond to the removal of the en ligands [calcd 12.77% (**1**), 12.77% (**2**), 12.68% (**3**)]. In the following weight loss, the three compounds continue to decompose gradually, and the resulting black unknown residues were found after complete decomposition.

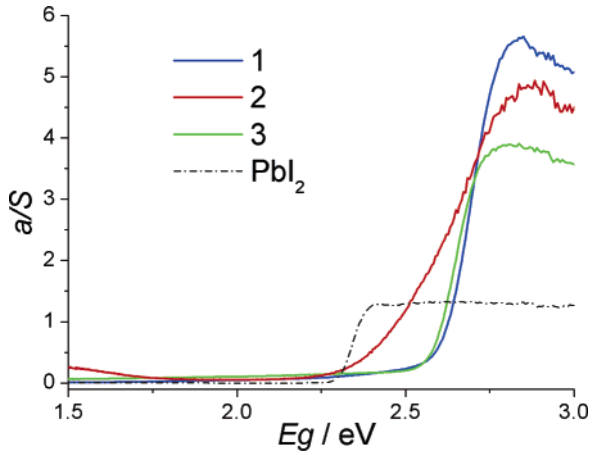

Figure 3. Optical absorption spectra for **1**−**3** and PbI_2.

Optical Properties. The optical absorption spectra of **1**−**3** and 2-D bulk PbI_2 have been measured by the diffuse-reflectance experiments. The absorption edges for **1**−**3** are of about 2.62, 2.45, and 2.59 eV, respectively, showing that the present compounds belong to semiconductors (Figure 3), which indicate a 0.2−0.3 eV blue shift of the absorption edges compared with the measured value of 2.30 eV for bulk PbI_2.

To evaluate and assign the observed spectra, we examine the linear optical response spectra of these compounds. The calculated imaginary $\epsilon_2(\omega)$ part of the frequency-dependent dielectric functions displayed in Figure 4 can be used to describe the real transitions between occupied and unoccupied bands.[21,26] There is only a feature peak (the first-absorption peak) below 8 eV for each compound (bulk PbI_2 and **1**−**3**) in the dispersion of the calculated $\epsilon_2(\omega)$ spectra. The peaks of 3.98, 4.36, 4.26, and 4.28 eV for bulk PbI_2 and **1**−**3**, respectively, are close to each other, although an ca. 0.3−0.4-eV peak shift for **1**−**3** in contrast with bulk PbI_2 is also observed. Accordingly, the first-absorption peaks for **1**−**3** can be assigned as the charge transfer within the inorganic iodoplumbate chains. The $[M(en)_3]^{2+}$ cation templates result in the assembly of the one-dimensional (1-D) iodoplumbate chains, which only have a perturbation effect on the adsorption of inorganic iodoplumbate chain but do not directly participate in the optical transition. The onset

(24) Chakravarthy, V.; Guloy, A. M. *Chem. Commun.* **1997**, 697.

(25) Saito, Y. *Inorg. Mol. Dissymm.* **1979**, 56.

(26) Zhang, Y. C.; Cheng, W. D.; Wu, D. S.; Zhang, H.; Chen, D. G.; Gong, Y. J.; Kan, Z. G. *Chem. Mater.* **2004,** *16*, 4150.

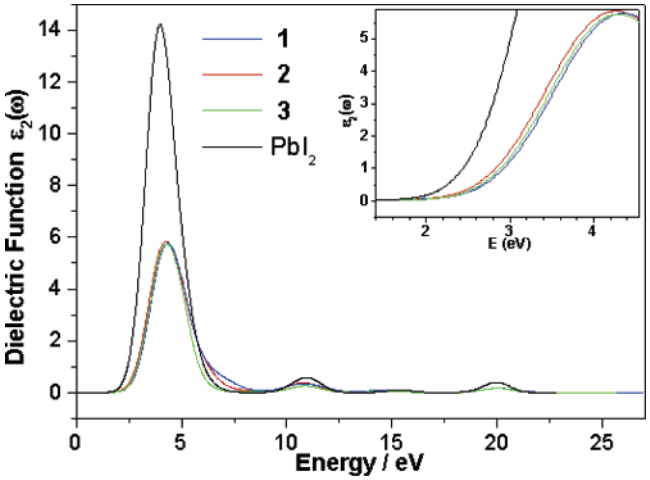

Figure 4. Calculated imaginary parts $\epsilon_2(\omega)$ of dielectric functions for the three compounds and bulk PbI_2.

of an effective transition edge shifts from 2.57 eV for bulk PbI_2 to 2.77, 2.68, and 2.74 eV for **1**−**3**, respectively, giving the same sequence of blue shifts as experimental results. The observed blue shift can be explained by the quantum confinement effect (QCE).[27] The change of kinetic energy due to the QCE will increase the band gap and the energy separation of allowed transitions near the absorption edge,[28] which is also seen in other hybrid semiconductors.[29,30]

On the other hand, it can be seen from the band structure and DOS (Figure 5) that the widths of the forbidden band of bulk PbI_2 and of the inorganic iodoplumbate chains in **1**−**3** are 2.29, 2.68, 2.59, and 2.63 eV, respectively, in agreement with the onset sequence of the imaginary parts of $\epsilon_2(\omega)$ of the dielectric function, as shown Figure 4, which proves again that the adsorption for **1**−**3** can be assigned as the charge transfer between the highest occupied molecular orbitals and the lowest unoccupied molecular orbitals of the inorganic iodoplumbate chain. In other words, there is no charge transfer occurring between the inorganic chains and the transition-metal complexes, in spite of the insertions of unpaired d orbitals of transition metals (Mn and Fe) into the forbidden band of the inorganic chains. The transition-metal complexes do not obviously alter the electronic structures of the iodoplumbate chains because of the noninteraction between the two moieties, which is also proven by the flat band of 3d orbitals of the transition-metal atoms. In terms of the partial DOS analyses, the absorption peaks for bulk PbI_2 and the hybrids are further assigned as charge transfers from Pb 6s I 5p occupied states to Pb 6p empty states.[28c,31]

Magnetic Properties. The magnetic susceptibilities of **1**, **2**, and **4** have been measured from ground crystals under a constant magnetic field of 5000 G over the temperature range of 2.0−300 K. The data are presented as plots of effective magnetic moment μ_{eff} vs T in Figure 6. The μ_{eff} value of **1** at 300 K is 5.78 μ_B, close to the 5.91 μ_B expected for the isolated spin-only $S_{Mn} = {}^5/_2$ ion.[32] Upon cooling, μ_{eff} slowly increases, reaches a maximum at $T = 70$ K ($\mu_{eff} = 5.82\ \mu_B$), and then decreases abruptly, suggesting weak ferromagnetic interactions among Mn(II) ions, as confirmed by the positive Weiss constant of 1.86 K via a nonlinear fit to data above 50 K. For **2**, the μ_{eff} value at 300 K is 5.94 μ_B, close to the 5.88 μ_B expected for the uncoupled spin-only system with $S_{Fe} = 2$ and $g_{Fe} = 2.4$.[33] The μ_{eff} value decreases slowly up to 50 K, following the rapid drop to 2.56 μ_B at 2 K, suggesting that the antiferromagnetic interaction exists in **2**, proven by the negative Weiss constant of −8.30 K via a similar fit. For **4**, μ_{eff} basically stays at 2.97 μ_B in most temperature ranges, compared with the 2.83 μ_B expected for the noninteraction spin-only $S_{Ni} = {}^1/_2$ ion, indicating the paramagnetic properties.

The same coordination environment of magnetic metal ions in **1**, **2**, and **4** leads to a comparable contribution of crystal-field energy to the magnetic state. The difference between the magnetic properties of **1** and **2** may mainly come from the dipole interaction and spin−orbit coupling. The through-space dipole−dipole interactions will, in general, favor a ferromagnetic state for dipole pairs,[34] and its Hamilton operator shows a relation to the square of the spin of metal ions,[35] resulting in the ferromagnetic state of **1**, in which the spin−orbit coupling of $S_{Mn} = {}^5/_2$ can be negligible. In contrast with **1**, compound **2** shows the antiferromagnetic state due to the larger spin−orbit coupling and weaker dipole interaction with $S_{Fe} = 2$.

The magnetic data of **1** were analyzed in terms of a model of single-ion zero-field splitting (ZFS). First, after taking into account the Zeeman perturbation and ZFS, a magnetic susceptibility equation can be obtained as follows:[16]

$$\chi_{Mn} = (\chi_z + 2\chi_x)/3 \qquad (1)$$

$$\chi_z = \frac{Ng_z^2\beta^2}{4kT}\frac{1 + 9\exp(-2D/kT) + 25\exp(-6D/kT)}{1 + \exp(-2D/kT) + \exp(-6D/kT)}$$

$$\chi_x = \frac{Ng_x^2\beta^2}{4kT}\frac{9 + 8kT/D - 11\exp(-2D/kT)/2(D/kT) - 5\exp(-6D/kT)/2(D/kT)}{1 + \exp(-2D/kT) + \exp(-6D/kT)}$$

where χ_{Mn} is the magnetic susceptibility in the absence of an exchange field and D is the ZFS parameter. Second,

(27) (a) Umebayashi, T.; Asai, K. *Phys. Rev B* **2003**, *67*, 155405. (b) Hong, X.; Ishihara, T.; Nurmikko, A. V. *Phys. Rev. B* **1992**, *45*, 6961. (c) Koutselas, I. B.; Ducasse, L.; Papavassiliou, G. C. *J. Phys.: Condens. Matter* **1996**, *8*, 1217. (d) Shimizu, M.; Fujisawa, J.-I.; Ishi-Hayase, J. *Phys. Rev B* **2005**, *71*, 205306. (e) Kondo, T.; Iwamoto, S.; Hayase, S.; Tanaka, K.; Ishi, J.; Mizuno, M.; Ema, K.; Ito, R. *Solid State Commun.* **1998**, *105*, 503. (f) Tanaka, K.; Ozawa, R.; Umebayashi, T.; Asai, K.; Ema, K.; Kondo, T. *Phys. E* **2005**, *25*, 378. (g) Azuma, J.; Tanaka, K.; Kamada, M.; Kanno, K. *J. Phys. Soc. Jpn.* **2002**, *71*, 2730.

(28) (a) Fu, H.; Zunger, A. *Phys. Rev B* **1998**, *57*, R15064. (b) Axtell, E. A.; Liao, J.-H.; Pikramenou, Z.; Kanatzidis, M. G. *Chem.—Eur. J.* **1996**, *2*, 656.

(29) (a) Henglein, A. *Chem. Rev.* **1989**, *89*, 1861. (b) Steigerwald, M. L.; Brus, L. E. *Acc. Chem. Res.* **1990**, *23*, 183. (c) Weller, H. *Adv. Mater.* **1993**, *5*, 88. (d) Hagfeldt, A.; Gratzel, M. *Chem. Rev.* **1995**, *95*, 49. (e) Fendler, J. H.; Meldrum, F. C. *Adv. Mater.* **1995**, *7*, 607. (f) Alivisators, A. P. *J. Phys. Chem.* **1996**, *100*, 13226.

(30) (a) Huang, X. Y.; Li, J.; Zhang, Y.; Mascarenhas, A. *J. Am. Chem. Soc.* **2003**, *125*, 7049. (b) Huang, X. Y.; Li, J. *J. Am. Chem. Soc.* **2000**, *122*, 8789. (c) Huang, X. Y.; Heulings, H. R., IV; Le, V.; Li, J. *Chem. Mater.* **2001**, *13*, 3754. (d) Heulings, H. R., IV; Huang, X. Y.; Li, J. *Nano Lett.* **2001**, *1*, 521. (e) Fu, H. X.; Li, J. *J. Chem. Phys.* **2004**, *120*, 6721. (f) Deng, Z. X.; Li, L.; Li, Y. D. *Inorg. Chem.* **2003**, *42*, 2331.

(31) Papavassiliou, G. C. *Prog. Solid State Chem.* **1997**, *25*, 125.

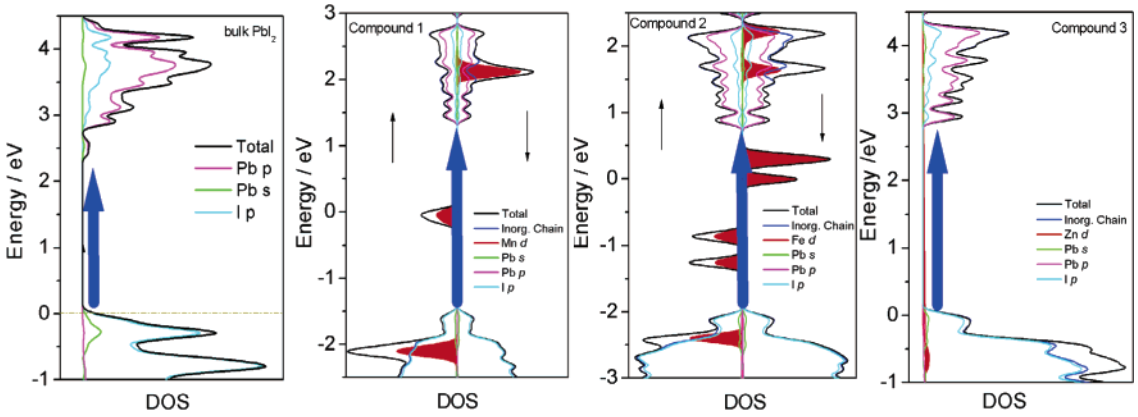

Figure 5. Total and partial DOS plots of bulk PbI_2 and **1**−**3** with the Fermi level setting as zero. The blue arrowheads represent the transfer from the highest occupied molecular orbital of iodoplumbate to the lowest unoccupied molecular orbital of iodoplumbate.

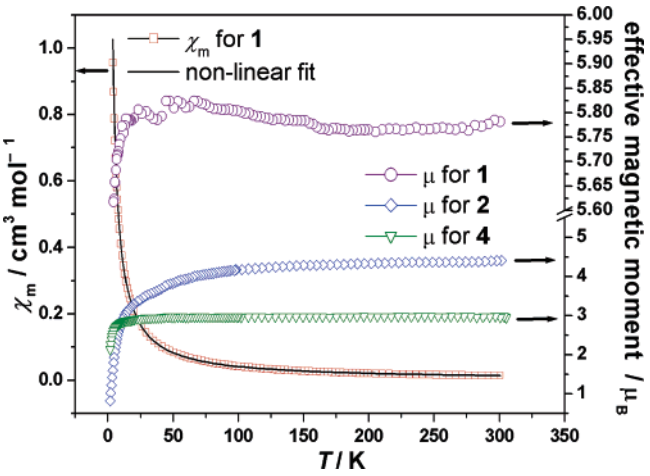

Figure 6. Plots of μ_{eff} vs T over the temperature range of 2−300 K at a field of 5000 G for **1**, **2**, and **4** and fitting of the variable-temperature magnetic susceptibility data of **1**.

because of the weak dipole interactions, expression (1) may be corrected based on the molecular field approximation, which is illustrated in eq 2,

$$\chi_M = \frac{\chi_{Mn}}{1 - 2zJ\chi_{Mn}/Ng^2\beta^2} \qquad (2)$$

where χ_M is the magnetic susceptibility actually measured, zJ is the exchange parameter for dipole interactions, and the rest of the parameters have their usual meanings. Fitting to eq 2 gives a set of the best-fitting parameters with $D = 0.993$ cm^{-1}, $g = 1.95$, and $zJ = 0.0083$ cm^{-1}, consistent with those reported.[36] An agreement factor defined as $R = \sum(\chi_m^{obs} - \chi_m^{cal})^2/\sum(\chi_m^{obs})^2$ is 9.0×10^{-5}. The positive zJ value, which is the exchange parameter for dipole interactions, also suggests that a weak ferromagnetic interaction exists in **1**. Similar fittings for **2** and **4** (Figures S4 and S5 of the Supporting Information) give $D_{Fe} = 0.35$ cm^{-1}, $g_{Fe} = 2.01$, and $zJ_{Fe} = -23.29$ cm^{-1} for the Fe(II) ion with $R = 3.0 \times 10^{-5}$ (above 100 K) and $D_{Ni} = 4.52$ cm^{-1}, $g_{Ni} = 2.10$, and $zJ_{Ni} = 0$ cm^{-1} for the Ni(II) ion with $R = 5.9 \times 10^{-10}$. The neglected rhombic parameter E for Fe(II) results in the derivation of the fitting curve under 100 K. The values of zJ for **2** and **4** prove their antiferromagnetic and paramagnetic properties again.

Conclusion

In conclusion, we have obtained novel magnetic semiconductors based on 1-D iodoplumbate nanowires to exhibit the magnetic and semiconducting properties simultaneously, which allows an easy assembly of the new type of hybrid magnetic semiconductor with a controllable size and a high degree of purity and uniformity through a conventional synthetic process. It is promising to obtain the magnetic semiconductors with promoted properties by selecting suitable magnetic metal−organic complexes and controlling the dimension and size of the inorganic components. Further studies are in progress in our laboratory.

Acknowledgment. We gratefully acknowledge the financial support of the NSF of China (Grant 20131020), the NSF for Distinguished Young Scientist of China (Grant 20425104), and the NSF of Fujian Province (Grant 2003I031) for support of this research.

Supporting Information Available: TGA curves and X-ray crystallographic files (CIF format) for the structure determination of **1**−**4**. This material is available free of charge via the Internet at http://pubs.acs.org.

IC051350V

(32) Wood, R. M.; Stucker, D. M.; Jones, L. M.; Lynch, W. B.; Misra, S. K.; Freed, J. H. *Inorg. Chem.* **1999**, *38*, 5384.
(33) Buschmann, W. E.; Miller, J. S. *Chem.—Eur. J.* **1998**, *4*, 1731.
(34) Wynn, C. M.; Girtu, M. A.; Brinckerhoff, W. B.; Sugiura, K.-I.; Miller, J. S.; Epstein, A. J. *Chem. Mater.* **1997**, *9*, 2156.
(35) Carlin, R. L. *Magnetochemistry*; Springer-Verlag: Berlin, 1986. $\mathbf{H} = \sum_{i,j}[u_i \cdot u_j/r_{ij}^3 - 3(u_i \cdot r_{ij})(u_j \cdot r_{ij})/r_{ij}^5]$ and $u = g\beta\mathbf{S}$.
(36) Lan, Y. H.; Kennepohl, D. K.; Moubaraki, B.; Murray, S. K.; Cashion, J. D.; Jameson, G. B.; Brooker, S. *Chem.—Eur. J.* **2003**, *9*, 3772.